Alternating morphology transitions in crystallization of NH_4Cl on agar plates

Ya-Fang Tu,[1] Rong-Bin Wei,[1] Jian-Ping Sang,[1,2] Sheng-You Huang,[1] and Xian-Wu Zou[1,*]
[1]*Department of Physics, Wuhan University, Wuhan 430072, China*
[2]*Department of Physics, Jianghan University, Wuhan 430056, China*

(Received 1 August 2007; revised manuscript received 25 February 2008; published 11 April 2008)

Two types of alternating morphology transitions have been observed in crystallization of NH_4Cl on agar plates. One is the alternating morphology transitions between dense branching morphology and sparse branching morphology, and the other is the alternating morphology transitions between dense branching morphology and zigzag branching morphology. The appearance of them is found to depend on the mass proportion of agar to NH_4Cl in the initial solution and the relative humidity. It is suggested that both the two alternating morphology transitions result from the oscillation of solute concentration in front of the growing interface caused by the competition of crystal growth and solute transfer at a moderate mass proportion. Which one of them occurs depends on the relative humidity, which controls the supersaturation.

DOI: 10.1103/PhysRevE.77.041601 PACS number(s): 81.10.Aj, 89.75.Kd, 64.70.K−, 81.30.−t

I. INTRODUCTION

Pattern formation in nonequilibrium systems is the subject of substantial fundamental and practical interests, and it has been intensively investigated during the past two decades. Well-known examples are viscous fingering [1,2], dielectric breakdown [3], growth of bacterial colonies [4,5], crystallization [6,7], and electrodeposition [8,9]. These systems exhibit similar morphologies, which are of three typical types: dendrite, fractal morphology, and dense branching morphology (DBM). Understanding the origin of these morphologies and looking for possible universal mechanisms are the most fascinating but challenging problems.

Up to now, much progress has been made towards the elucidation of these universal mechanisms, and a few unique morphologies were also found. One example is the zigzag pattern [10,11], which is obtained by the crystallization of NH_4Cl in a thin layer of agar gel sandwiched between two glass plates. Another example is the periodic patterns, which are often seen in nature and in many branches of science, such as the annual growth rings in plants and Liesegang rings. Periodic patterns have been observed in the growth of bacterial colonies and in the crystallization of $HgCl_2$ on the agar plate. The former was explained by the cyclical growth of a colony with alternative migration phase and consolidation phase [5], while the latter one was considered as periodic crystallization caused by a drying front during the evaporation [12,13]. When performing crystallization of NH_4Cl on the agar plate [14], a few periodic rings were also found during the growth of the DBM pattern, and it was explained by the variation of growth velocity. It seems that these periodic patterns are generated by repeated growth and rest of the crystal or the bacterial colony, and not any morphological transitions were illuminated in these periodic patterns.

Morphology transitions have been frequently observed in quasi-two-dimensional electrodeposition experiments, they are well known as the Hecker effect which is generally described as a sudden change in color and number of branches of the growing deposit [15–21]. It is widely accepted that the changes result from the interaction of the growing deposit with different chemical fronts advancing from the anode towards the cathode. So the change in the morphology appears at the same time on an envelope which reproduces the shape of the anode and one does not observe an oscillating behavior between two different morphologies. Also, alternating morphology transitions between dendrite and DBM have been found in the quasi-two-dimensional electrodeposition of $FeSO_4$ aqueous solution [22]. This transition occurs on each deposit branch independently, which is unlike the Hecker effect. It was explained to result from the periodic accumulation and depletion of H^+ impurities in front of the growing interface. For crystallization, morphology transition from dendrite to DBM has been observed in the final stages of the growth of alkali halides from solution [7]. This was ascribed to the change of concentration profiles caused by the decrease of drop thickness during the last stages of evaporation. However, up to now, there are not any reports about alternating morphology transitions in crystallization to our knowledge. Investigation on self-organized alternating morphology transitions should be very useful for understanding the formation mechanisms of different morphologies in nonequilibrium systems.

In this paper, we report our discoveries on two types of alternating morphology transitions, which generate patterns with repeated stripe structure, in the crystallization of NH_4Cl on agar plates. Our attention is focused on their transition process, growth conditions, relationships with normal morphologies and formation mechanisms. In these morphology transitions, the changes of branches happen simultaneously on an envelope, so they are different from the alternating morphology transitions in the electrodeposition of $FeSO_4$. On the other hand, the transitions are continuously repeated, and do not just happen in the final stages of crystallization, so they also differ from the previously mentioned Hecker effect and the morphology transitions in the crystallization of alkali halide. Therefore, there could be some different underlying mechanisms, and the investigation on that would be helpful to understand the crystallization dynamics under a complex condition.

*Corresponding author; xwzou@whu.edu.cn

II. EXPERIMENTAL PROCEDURE

The experiment was carried out on a thin film of agar gel containing NH_4Cl with a free surface, mounted on a glass substrate. Agar is a marine polysaccharide, often used as the model biopolymer in gelation. The agar molecules form a network, and water molecules are enclosed in the network. The density of the network can be controlled by the agar concentration [23].

The gel was prepared by dissolving agar into deionized hot water with concentration (C_a) varying from 0.2 wt % to 4.0 wt %. NH_4Cl (A.R. grade, 99.9%) was added thereafter and its concentration (C_N) was also in the range of 0.2 wt % to 4.0 wt %. 0.15 ml of the hot solution was dropped on a piece of glass slide (7.5×2.5 cm^2) and was spread uniformly to cover the area of 6×2.5 cm^2. The thickness of the gel thus prepared was about 100 μm for all runs. The glass slide was quickly placed into a small petri dish, which then was sealed. After being left at room temperature for about half an hour, the gel became compact. Then the glass slide with the gel on it was taken out from the dish and placed into a growth chamber. As the water in the gel medium gradually evaporated, the NH_4Cl solution became saturated first from the surface. Thus, the crystallization began on the surface of the thin agar plate. The evaporation rate was controlled by adjusting the relative humidity (RH) in the chamber from 20% to 80% and the temperature was kept at 23 °C.

The aggregates formed were observed by an optical microscope (BX51, Olympus, Japan) with a charge-coupled device (CCD) video system attached to it, and were further investigated by an atomic force microscope (AFM) (SPM-9500J3, Shimadzu, Japan) in tapping mode.

III. MORPHOLOGY CHARACTERISTICS OF THE PATTERNS FORMED BY ALTERNATING MORPHOLOGY TRANSITIONS

The macrograph of an aggregate with repeated stripe structure is shown in Fig. 1(a) which is captured by a digital cameral with black background. There are more than twenty stripes in the picture. In fact, the repeated stripes can extend through the whole sample except the edges where the thickness of gel becomes thin. By taking the optical micrograph, we found that these repeated stripes can be divided into two types according to the morphologies at small scale. One is an alternating dense-sparse branching pattern formed by alternating morphology transitions between a dense branching morphology and a sparse one (alternating dense-sparse transitions) [see Fig. 1(b)], and the other is an alternating dense-zigzag one formed by alternating morphology transitions between a dense branching morphology and a zigzag branching morphology (alternating dense-zigzag transitions) [see Fig. 1(c)]. The dense branching morphology is characterized by unstable tips, but with a stable flat growth front and a homogeneous filling of space. The sparse branching morphology is formed by the continuous growth of just a few branches of the previously grown DBM, and the newly grown branches are spaced sparser than that of DBM. The sparse branching region corresponds to the dark lines in Fig. 1(a). The zigzag branching morphology shows a random and ramified morphology at a large scale, but each branch consists of regularly shaped crystallites. In spite of the differences between the two morphologies, the zigzag branching morphology is also sparse in analogy to the sparse branching one, so the macrograph of the aggregate formed by alternating dense-zigzag transitions is similar to that of the alternating dense-sparse ones. In general, the alternating dense-zigzag transitions appear in a condition with larger humidity than that of the alternating dense-sparse transitions.

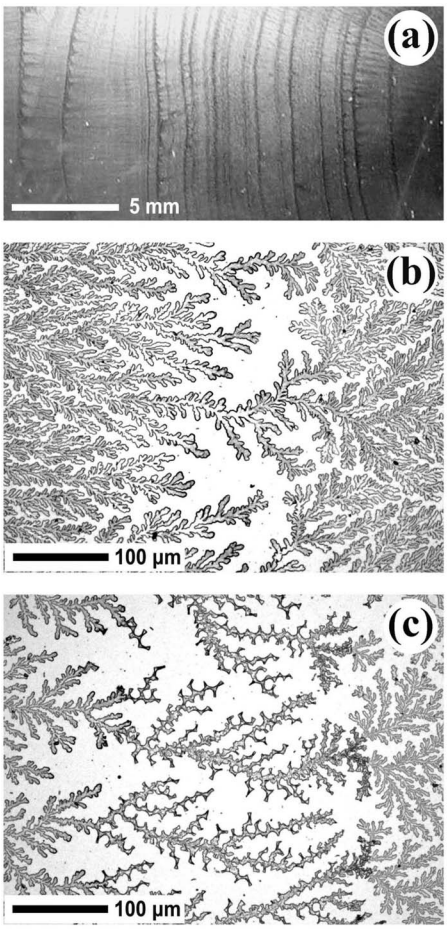

FIG. 1. Patterns of the crystallite aggregate of NH_4Cl. (a) The macrograph of an aggregate with repeated stripe structure. Because a black background is used, the light region corresponds to the compact part of the aggregate and the dark region corresponds to the sparse part. (b) The optical micrograph of the aggregate showed in (a). It shows the alternating dense-sparse transitions. (c) The optical micrograph of another aggregate with similar repeated stripe structure. It shows the alternating dense-zigzag transitions. The initial concentrations of NH_4Cl and agar are 0.2 wt % and 0.4 wt %, respectively. The relative humidity for crystal growth is 40% for (a) and (b), 58% for (c), respectively.

IV. TRANSITION PROCESS OF THE ALTERNATING MORPHOLOGY TRANSITIONS

Figure 2 illustrates a typical growing process from a dense branching morphology to a sparse one, and then back to a dense one (alternating dense-sparse transitions). Figures

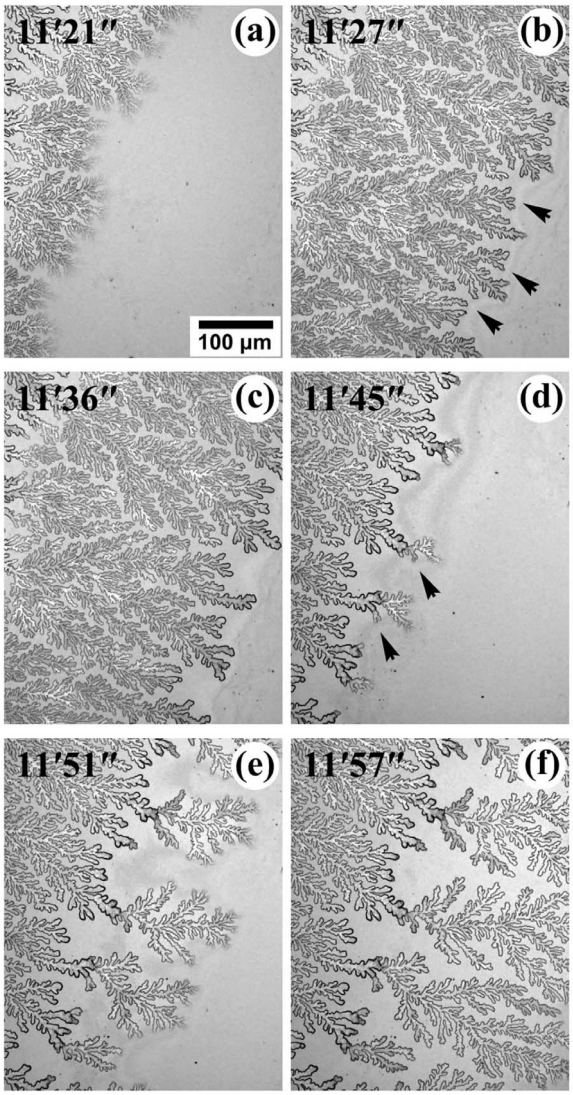

FIG. 2. *In situ* optical micrographs demonstrating the morphological evolution from a dense branching morphology [(a) and (b)] to a sparse one [(c), (d), and (e)], and then back to a dense one (f). By comparison with the viewing field of (c), that of (d) is shifted 200 μm to the right. The digits in the upper-left corner of each frame stand for minutes and seconds. In (b) and (d), the branches shown by arrows grow very slowly and ultimately stop growing, in spite of their open neighborhood. The initial concentrations of NH_4Cl and the agar are 0.4 wt % and 0.6 wt %, respectively. The relative humidity for crystal growth is 40%.

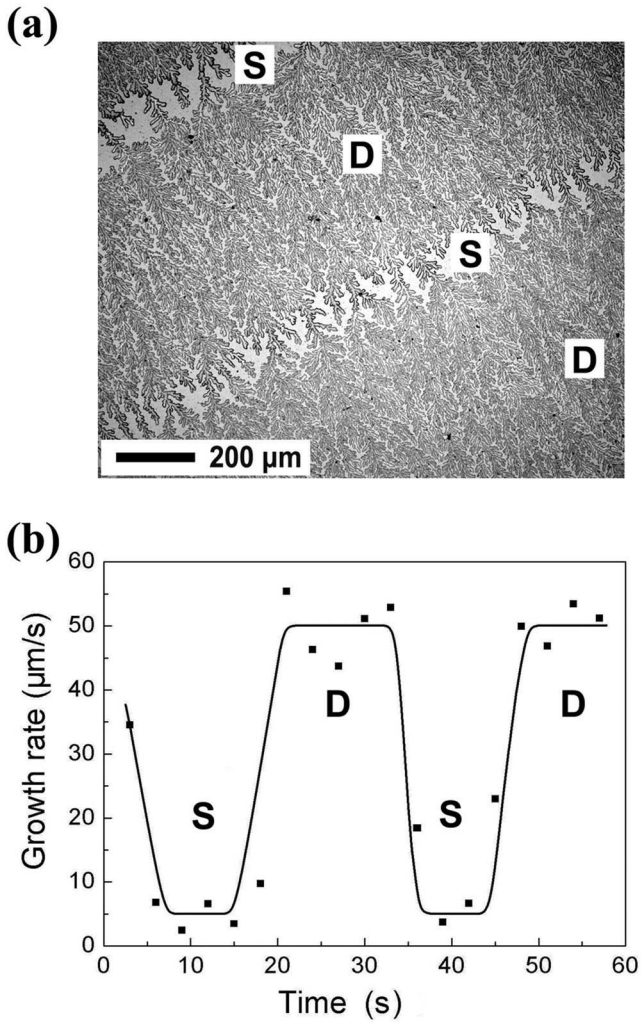

FIG. 3. (a) The optical micrograph of an aggregate formed by alternating dense-sparse transitions, which develops from the upper-left corner towards the lower-right one. (b) The interfacial growth rate measured as a function of time during the morphology transitions in (a). The dense and sparse branching morphologies are marked as *D* and *S*, respectively. The black squares indicate measured values. The initial concentrations of NH_4Cl and the agar are 0.4 wt % and 0.6 wt %, respectively. The relative humidity for crystal growth is 40%.

2(a) and 2(b) show the DBM growth. In this case, the aggregate grows very fast. At the end of the DBM growth, only a few protrudent tips continue growing and most of the tips almost stop developing. These obsolescent tips are marked by the arrows in Fig. 2(b). Those protrudent tips split, grow out, and develop into a sparse branching morphology, as shown in Figs. 2(c)–2(e). At the stage of the sparse branching morphology, the aggregate grows very slow. By the end of the sparse branching growth, the growth rate of the tips at the growing front increases and they develop into the dense branching morphology again [see Fig. 2(f)]. It can be seen that the growth of branches in the sparse branching zone shows a strong screening effect [24], that is, a few branches screen the growth of the others. This screening effect is a prominent feature of fractal morphology which is described by the diffusion-limited aggregation model [25]. Thus, the sparse branching morphology can be considered as a variation of the fractal morphology.

The growth rate is measured during the alternating dense-sparse transitions, as shown in Fig. 3. Figure 3(a) shows the micrograph of the aggregate formed by alternating dense-sparse transitions, and Fig. 3(b) plots the relationship between the corresponding growth rate and growth time. The growth rate of the aggregate is defined as the average envelope moving rate. It can be seen that the DBM grows faster than the sparse branching morphology, and the growth rate suddenly jumps during the transitions. The growth of the sparse branching morphology is slow, but its growth time can

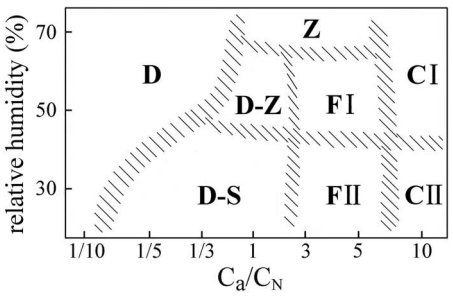

FIG. 4. Morphological phase diagram of NH_4Cl aggregate when varying the mass proportion of agar (C_a) to NH_4Cl (C_N) in the initial solution and the relative humidity. *D*: dense branching morphology; *Z*: zigzag pattern; *D-Z*: alternating dense-zigzag branching pattern; *D-S*: alternating dense-sparse branching pattern; *F*I: fractal I; *F*II: fractal II; *C*I: cluster I; *C*II: cluster II.

be comparable to that of the dense one, so the sparse branching zones are narrow.

The growing process of the alternating dense-zigzag transitions is similar to that of the dense-sparse transitions. In the case of the dense-zigzag transitions, the dense branching growth and zigzag branching growth take place in turn, and the growth rate of the zigzag branches is also much lower than that of the dense branches.

V. MORPHOLOGICAL PHASE DIAGRAM AND THE RELATIONSHIP AMONG VARIOUS PATTERNS

To clarify the growth conditions of the two alternating morphology transitions, and to find out the relationship between the formed two patterns and others previously reported, overall investigations with various experimental conditions were carried out. It was found out that the mass proportion of agar to NH_4Cl and the relative humidity were the key factors to determine the morphologies of the NH_4Cl aggregate. The results are shown in Fig. 4. There exist eight typical patterns in this morphological phase diagram. They are the dense branching morphology (*D*), zigzag pattern (*Z*), alternating dense-zigzag branching pattern (*D-Z*), alternating dense-sparse branching pattern (*D-S*), fractal I (*F*I), fractal II (*F*II), cluster I (*C*I) and cluster II (*C*II). Corresponding optical micrographs of them are shown in Fig. 5.

By just varying the initial agar and NH_4Cl concentrations, Yasui and Matsushita [14] obtained a morphological phase diagram of NH_4Cl crystals. Five typical patterns were displayed, which are crosslike regular dendritic, regular DBM, random DBM, diffusion-limited aggregration (DLA), and compact patterns. The compact patterns and DLA are respectively similar to the cluster II and fractal II observed in our system. The random DBM pattern is similar to the DBM in our morphological phase diagram. The regular dendrite and regular DBM are also observed by us in very small mass proportion of agar to NH_4Cl. In the case of no agar gel, the aggregate also appears as regular dendrite. Compared to the random DBM and the other morphologies, the two regular morphologies have some main branches, which indicates that the anisotropy plays an important role in the formation of these regular morphologies. These two regular morphologies

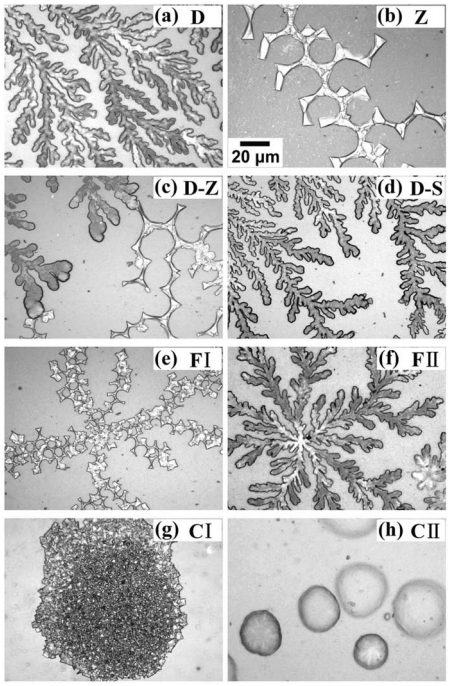

FIG. 5. Optical micrographs showing the various types of patterns grown in corresponding regions of Fig. 4. (a) DBM (C_a=0.2, C_N=0.6, RH=58%), (b) zigzag pattern (C_a=0.6, C_N=0.6, RH =70%), (c) alternating dense-zigzag branching pattern (C_a=0.4, C_N=0.2, RH=50%), (d) alternating dense-sparse branching pattern (C_a=0.6, C_N=0.6, RH=30%), (e) fractal I (C_a=0.6, C_N=0.2, RH =58%), (f) fractal II (C_a=0.6, C_N=0.2, RH=30%), (g) cluster I (C_a=2.0, C_N=0.2, RH=58%), (h) cluster II (C_a=2.0, C_N=0.2, RH=28%).

are not shown on the phase diagram because what we care about mostly in this paper are the morphologies which are strongly affected by the random perturbations from the gel, and the transitions among them.

As it is shown in Fig. 4, when the mass proportion of agar (C_a) to NH_4Cl (C_N) in the initial solution is small (region *D*), DBM is obtained, an example of which is shown in Fig. 5(a). In this region, the width of branches increases with the increase of relative humidity.

Increasing the mass proportion, and with a very high relative humidity, zigzag pattern is formed (region *Z* of Fig. 4). One zigzag branch is shown in Fig. 5(b), and a lower magnification of the zigzag pattern will be shown later in Fig. 7(c). In the system where the zigzag pattern was first observed [10], the evaporation of water was very slow, which corresponds to the high relative humidity condition in our experimental system. Decreasing the relative humidity, fractal-like patterns are formed (regions *F*I and *F*II). Corresponding micrographs are shown in Figs. 5(e) and 5(f), respectively. Both of these two patterns have the characteristics of fractal morphology, but the former has zigzag branches, and the latter has branches similar to that of the DBM. Thus, we named them fractal I and fractal II, respectively.

When the initial concentration of agar is much higher than that of the NH_4Cl, the pattern becomes compact and rounded clusterlike patterns are obtained. In this case, when the relative humidity is high (region *C*I), the cluster seems to be

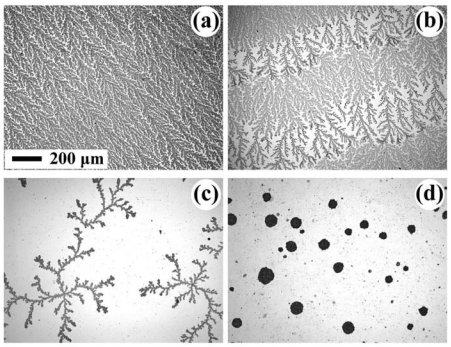

FIG. 6. Optical micrographs showing the morphology evolution of NH_4Cl crystals when the mass proportion in the initial solution (C_a/C_N) is varied from 1/3 to 10 and the relative humidity (RH) is fixed at 58%. (a) Dense branching morphology (C_a=0.2, C_N=0.6, C_a/C_N=1/3), (b) alternating dense-zigzag branching pattern (C_a=0.4, C_N=0.2, C_a/C_N=2), (c) fractal I (C_a=0.6, C_N=0.2, C_a/C_N=3), (d) cluster I (C_a=2.0, C_N=0.2, C_a/C_N=10).

formed by the piling up of a great deal of small crystallites [see Fig. 5(g)]. It evolves from the zigzag pattern and fractal I, so it has a jagged boundary like that of the zigzag pattern and fractal I. When the relative humidity is low (region *C*II), the cluster appears as a compact pie with circular shape and has a rough surface [see Fig. 5(h)]. Since it evolves from fractal II, it has a gently curved boundary similar to that of the DBM and fractal II. Therefore, we named them cluster I and cluster II, respectively. The cluster I is similar to the Eden cluster obtained by two-dimensional computer simulation based on the Eden model [26]. As to cluster II, since it appears as a compact pie, it can also be considered similar to the Eden cluster in essence. Increasing the mass proportion even further, crystals do not appear even after several days, which is the same as that found in Ref. [14].

The alternating dense-zigzag branching pattern is found to grow in the region *D*-*Z*, which is located between the regions *D* and *F*I, and the alternating dense-sparse branching pattern appears in the region *D*-*S*, which is situated between the regions *D* and *F*II. The closeup optical micrographs of the two patterns are shown in Figs. 5(c) and 5(d), respectively. In addition, a variation in the alternating morphologies is observed when changing the value of C_a/C_N in the *D*-*S* or *D*-*Z* regions. With the decrease of C_a/C_N in the *D*-*S* or *D*-*Z* regions, the length of one period of morphology alternation becomes longer and fewer stripes appear on one sample.

Our experiments show that the growth rates of various morphologies are also different. For example, the DBM can extend over the glass slide in several minutes with a growth rate of about 100 μm/s when the relative humidity is about 50%, while more than two hours are required for cluster I to start crystallization. In general, the larger the mass proportion (C_a/C_N), or the higher the relative humidity (RH), the lower the growth rate.

The effects of the mass proportion and the relative humidity on the morphologies of the NH_4Cl aggregate are investigated, respectively. First, the morphology evolution when just increasing the mass proportion is shown in Fig. 6. It shows that when the relative humidity is fixed at an intermediate value (here, RH=58%), and the mass proportion is varied from 1/3 to 10, the morphology appears as DBM, dense-zigzag branching pattern, fractal I and cluster I, in sequence. Our experiments also show that accompanying this morphology evolution, the rate of nucleation increases, and the growth rate of crystallite decreases. Then, the morphology evolution of NH_4Cl crystals as the RH increases is shown in Fig. 7. It illustrates that when the mass proportion of agar to NH_4Cl in the initial solution is fixed at a certain value (here, C_a/C_N=3), and the relative humidity is varied from 30% to 70%, the morphology changes from fractal II to fractal I and then to the zigzag pattern. The zigzag pattern in Fig. 7(c) is shown at a lower magnification. The fractal I pattern has much smaller size than the zigzag pattern despite that both of them possess zigzag branches. While many small fractal patterns appear simultaneously on the substrate in the region *F*I and *F*II, one large zigzag pattern can grow throughout the substrate in the region *Z*. Moreover, the lower magnification of the fractal II is similar to that of fractal I. Thus, the crystals grown in region *F*I show much more similarities with that in region *F*II than that in region *Z*, and this is the reason why we named the pattern in region *F*I the fractal I but not zigzag II.

VI. PARTITION ON THE MORPHOLOGICAL PHASE DIAGRAM FROM THE MACROSCOPICAL AND MICROSCOPICAL POINTS OF VIEW

The microscopic surface morphologies of various NH_4Cl aggregates were further studied by AFM. The pictures of the dense-zigzag branching pattern are taken as a representative (see Fig. 8). Figure 8(a) presents a full view of the morphology transition from a dense branching morphology to a zig-

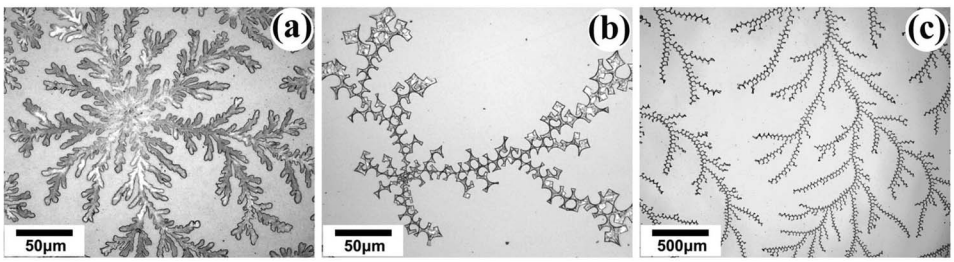

FIG. 7. Optical micrographs showing the morphology evolution of NH_4Cl crystals when the relative humidity (RH) is varied from 30% to 70% and the mass proportion in the initial solution (C_a/C_N) is fixed at 3. (a) Fractal II (C_a=0.6, C_N=0.2, RH=30%), (b) fractal I (C_a=0.6, C_N=0.2, RH=52%), (c) zigzag pattern (C_a=0.6, C_N=0.2, RH=70%).

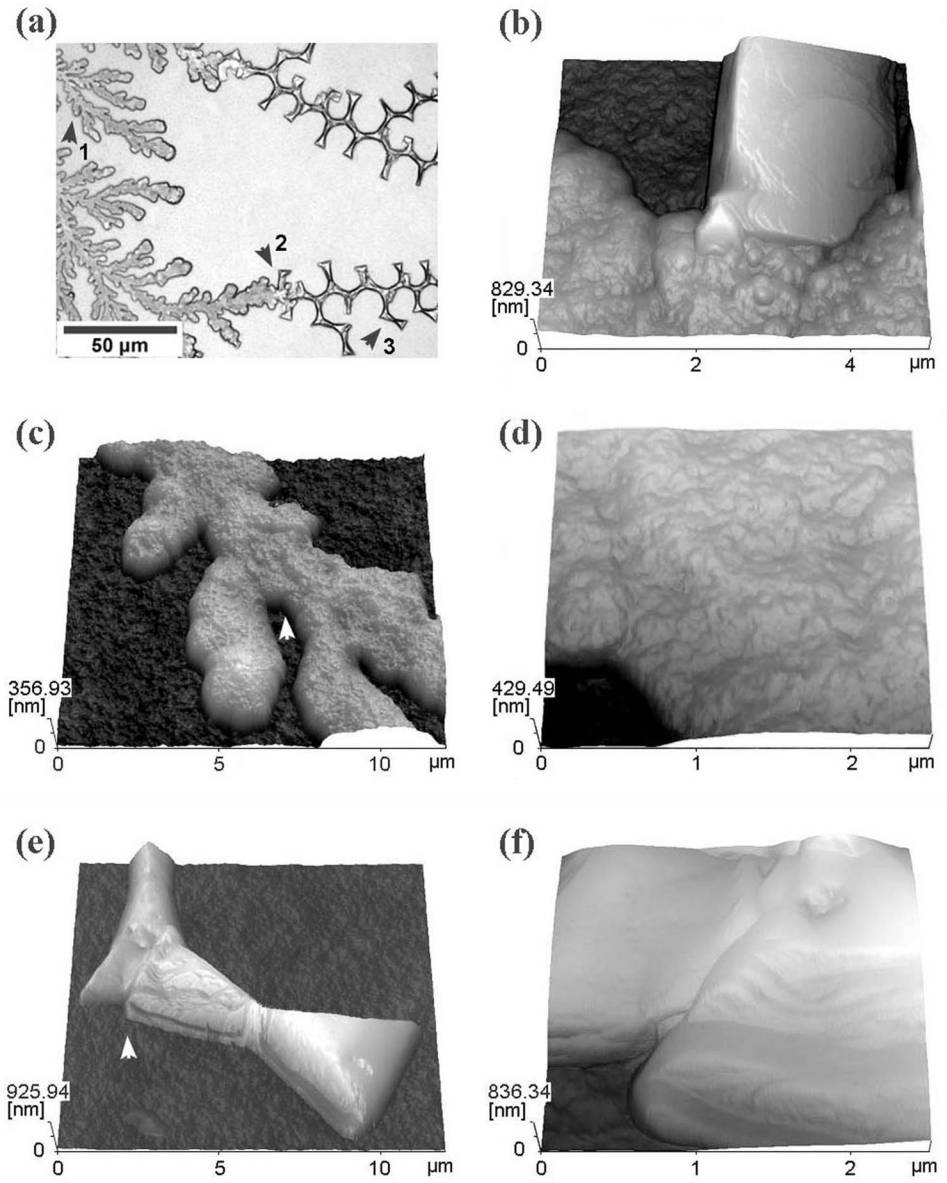

FIG. 8. Optical micrograph (a) and AFM micrographs (b)–(f) of the morphology transition of NH_4Cl crystals from a dense branching morphology to a zigzag branching morphology. (a) A full view of the morphology transition from DBM to the zigzag branching morphology. (b) AFM micrograph of the surface of the transition region from DBM to zigzag branching morphology, corresponding to the region pointed by the arrow 2 in (a). (c) AFM micrograph of the DBM part, corresponding to the region pointed by the arrow 1 in (a). (d) AFM micrograph of the detailed surface morphology of the region pointed by the white arrow in (c). (e) AFM micrograph of the zigzag part, corresponding to the region pointed by the arrow 3 in (a). (f) AFM micrograph of the detailed surface morphology of the region pointed by the white arrow in (e). The growth condition is C_a=0.6, C_N=0.6, and RH=50%.

zag branching morphology. Figures 8(c) and 8(d) are the AFM micrographs of the surface of the DBM part, Figs. 8(e) and 8(f) are that of the zigzag part. It can be seen that the surface of DBM is very rough. In contrast, the surface of the zigzag branch is smooth and faceted. In the zigzag part, bunched steps can be clearly observed on the side face of the crystallites, which is consistent with the results of previous research [10]. A closer view of the transition region is shown in Fig. 8(b), from which the difference in surface morphologies between the DBM and zigzag part can be clearly seen. In addition, both fractal I and the zigzag pattern have zigzag branches with smooth surface as the zigzag branching morphology has, and fractal II has the branching morphology with rough surface as DBM has. As to cluster I and cluster II, the AFM pictures of their surfaces are shown in Fig. 9. It can be seen that cluster I has the same smooth surface as zigzag branching morphology, and cluster II has the same rough surface as DBM.

To sum up, based on the macroscopic morphological features, the morphologies of NH_4Cl aggregate could be divided into three types: DBM, fractal, and cluster. Thus we can propose a partition of the previous morphological phase diagram. In Fig. 10(a), three new regions are differentiated by different colors, and the blank represents the transition zone where the two alternating morphology transitions occur. So both the alternating dense-zigzag transitions and the alternating dense-sparse transitions can be considered as alternating morphology transitions between DBM and fractal. In detail, alternating dense-zigzag branching pattern (*D-Z*) is formed by alternating morphology transitions between DBM and fractal I (fractal I has zigzag branches), and the alternating dense-sparse branching pattern (*D-S*) is formed by alternating morphology transitions between DBM and fractal II (in a sense, the sparse branching morphology can be considered as a variation of fractal II). On the other hand, according to the characteristics of the microscopic surface morphology, the NH_4Cl aggregates could be divided into two types: rough and smooth surface. Based on the surface feature, another partition on the morphological phase diagram is shown in Fig. 10(b). It can be seen that *D-Z* is formed by alternating

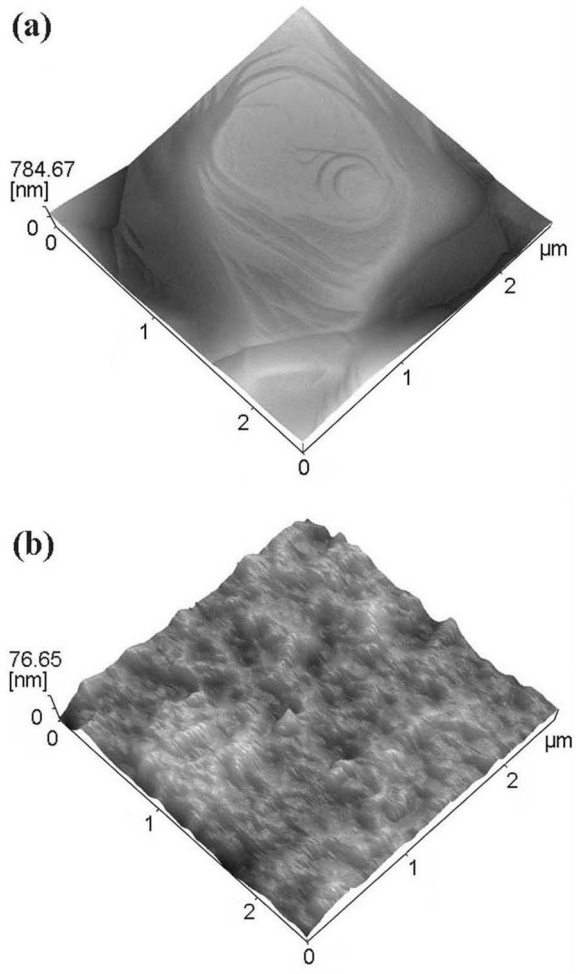

FIG. 9. AFM micrographs of the surface of cluster I and cluster II. (a) Cluster I and (b) cluster II.

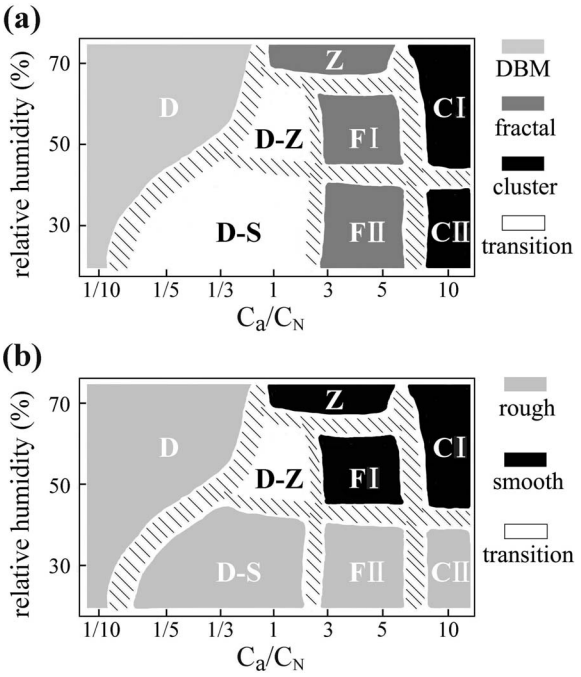

FIG. 10. Partitions on the morphological phase diagram from a macroscopical and a microscopical point of view, respectively. (a) According to the macroscopic morphological features, there exist three regions: DBM, fractal, and cluster. (b) According to the characteristics of the microscopic surface morphology, there exist two regions: rough and smooth surface. The blank region is the transition zone in which two phases coexist. The capital letters *D*, *Z*, *S*, *F*, and *C* represent dense, zigzag, sparse, fractal, and cluster, respectively.

transitions between the smooth surface growth and rough surface growth, but *D-S* still belongs to the rough surface growth.

VII. FORMATION MECHANISM OF THE DIFFERENT MORPHOLOGIES AND THE ALTERNATING MORPHOLOGY TRANSITIONS

As a general rule, different growth patterns are determined by the interplay between macroscopic driving force and microscopic interfacial dynamics [27]. It can be seen that the distribution of different regions in Fig. 10(a) mainly depends on the value of C_a/C_N, that is, with the increase of the mass proportion (C_a/C_N), the morphology changes from DBM to fractal then to cluster. It indicates that such a distribution, which is divided according to the macroscopic morphological features, is controlled by a macroscopic solute transport dynamics. In present experiments, the solute transport is mainly controlled by the mass proportion of agar to NH_4Cl in the initial solution. Crystallization of NH_4Cl in our system is realized by the evaporation of water. As time passes, both concentrations of agar and NH_4Cl gradually increase every moment. When the NH_4Cl solution becomes supersaturated, crystallization begins. Compared to the time taken for NH_4Cl to begin crystallization, the completion of crystallization takes a very short time. So the changes in concentrations of agar and NH_4Cl during the process of crystallization can be neglected in our experiment. Considering that the mass proportion of agar to NH_4Cl in the solution will be kept unchanged, the higher the initial mass proportion is, the higher the concentration of agar gel is when crystallization begins. As mentioned in Sec. II, the agar molecules form a network and the density of the network increases with the agar concentration. So with the increase of the agar concentration, convection is suppressed, and diffusion will be the only mechanism available for the supply of solute to the growing crystal [28]. Besides, the diffusion coefficient of solute also decreases with the increase of agar concentration [28,29]. Therefore, the larger the mass proportion, the higher the agar concentration, and the harder the solute transport. Moreover, as proposed by Yasui and Matsushita [14], the gel with random network structure plays a role of random perturbations for crystal growth, and the degree of perturbations is stronger with larger agar concentration. Thus, the distribution of regions in Fig. 10(a) can be explained as follows. In the case of no agar gel, the solute diffuses easily and is amply supplied in front of the growing interface. The aggregate grows up very fast and appears as dendrite morphology with strong anisotropy, which is a very common morphology from normal aqueous solution. In the case of small mass

proportion, the agar concentration is low and the solute is well supplied, so the aggregate grows up quickly. However, the anisotropy which stabilizes the dendrite growth is reduced by the random external perturbations from the gel. Thus, random tip-splitting dominates the growth, and a DBM is formed. In the case of intermediate mass proportion, the agar concentration is intermediate, solute transport is limited by diffusion, so the aggregate appears as fractal morphology. The growth of fractal morphology is also governed by random tip splitting, but its growth rate is about 10 times less than that of DBM. Thus, nucleation takes place simultaneously at many places of the slide, each nucleus grows into a fractal aggregate, and many fractals eventually spread over the slide. Particularly, in the case of large mass proportion, the agar concentration is rather high. As a result, the solutes diffuse very slowly. In the ideal diffusion-limited aggregation, a deposited adatom diffuses randomly on the surface, and once it hits an island it is trapped without further diffusion. However, during real growth, the adatom reaching an island will attempt to relax to a lower energy site by diffusion along the island edge. When the edge diffusion becomes faster than the rate at which an adatom reaches the island, a fractal-to-compact morphology transition takes place [30–33]. Also, if the edge diffusion barrier is sufficiently low, the atoms can visit many edge sites of an island. Then all edge sites can grow with an equal probability which is similar with the Eden growth model, and thus the island shape will be similar to an Eden cluster [34]. Therefore, in the case of large mass proportion in our experiment, as the rate of diffusion decreases further, the adatoms will have sufficient time to relax locally along the island edges before the arrival of a new adatom, thus a compact island similar to an Eden cluster is obtained.

In Fig. 10(b), the distribution of the two regions based on the characteristics of microscopic surface morphology is considered to be controlled by microscopic interfacial growth kinetics. It can be seen that when the relative humidity is lower than 50%, fractal I and cluster I with smooth surfaces are replaced by fractal II and cluster II with rough surfaces, respectively. The transition from smooth to rough interface is regarded as a kind of phase transition, and it is termed as "roughening transition"[35–40]. It is well known that thermal roughening transition occurs when the temperature becomes higher than a critical value, while kinetic roughening transition takes place at a sufficiently large supersaturation when the temperature is below the thermal roughening temperature [36–38]. In present case, temperature is fixed and the surface morphology changes with the relative humidity, so the roughening transition is a kinetic roughening transition. Many researches on crystallization from solution have found that when the supersaturation exceeds a critical value, kinetic roughening takes place, which makes the surface structure changes from smooth to rough [39,40]. In our experiment, the supersaturation for NH_4Cl crystal growth is mainly controlled by the evaporation rate of water and solute concentration in front of the growing interface. The less the relative humidity, the larger the evaporation rate is, then the larger the supersaturation is. On the other hand, the smaller the mass proportion of agar to NH_4Cl is, the better the solute supply is, then the larger the supersaturation is. According to this, the distribution of regions in Fig. 10(b) can be explained as follows. When the mass proportion is smaller ($C_a/C_N<1/2$), the supersaturation is larger than the critical value for kinetic roughening because of the well-supplied solute. As a result, the aggregate appears as DBM or dense-sparse branching pattern, both of which belong to the rough surface growth. In the case of larger mass proportion ($C_a/C_N>1/2$), the larger agar concentration obstructs water from evaporation, and the solute is ill supplied. These factors are unfavorable for raising supersaturation. Therefore, only when the relative humidity is less than 50%, the supersaturation can be larger than the critical value for kinetic roughening, and the aggregate appears as alternating dense-sparse branching pattern, fractal II and cluster II, which belong to the rough surface growth. Otherwise, it appears to be zigzag pattern, fractal I and cluster I, which belong to the smooth surface growth.

As stated in Sec. VI, both of the alternating dense-zigzag transitions and the alternating dense-sparse transitions can be essentially considered as alternating transitions between DBM and fractal. Since DBM results from a well supplied growth at a small mass proportion and fractal morphology is formed by the diffusion-limited aggregation at an intermediate mass proportion, the alternating morphology transitions between DBM and fractal is considered to be caused by the oscillation of the solute concentration in front of the growing interface at a moderate mass proportion. It has been observed in many systems that the solute concentration in front of the growing interface oscillates when the competition of crystal growth and solute transfer becomes very strong [41–43]. In regions *D*-*S* and *D*-*Z* in Fig. 4, at the beginning of the experiments, since solutes near the growing interface are sufficient, the deposit has a DBM morphology and the system belongs to region *D*. With the growth of DBM aggregate, solutes in front of the growing interface are consumed, however, the transport of solutes towards the growing interface is too slow to compensate the local depletion of solute concentration. Therefore, the solute concentration in front of the growing interface declines. Due to the local decrease of C_N, then of the local increase of C_a/C_N, the system locally moves horizontally in the diagrams shown in Fig. 4, and enters region *F*II and *F*I, respectively. The deposit morphology then switches from DBM to sparse or zigzag branching morphology, respectively. During the slower growth of the fractal-like branches, the rate of solute consumption is lower than that of solute transfer. Consequently, solute in front of the growing interface increases and fast DBM growth comes back. This process repeats and thus alternating dense-sparse transitions and alternating dense-zigzag transitions take place. This suggested mechanism is compatible with our experimental data. Since lower agar concentration leads to a better solute supply in front of the growing interface, when decreasing the value of C_a/C_N in the *D*-*S* and *D*-*Z* regions, the DBM will grow longer, and the morphology transitions will take place less frequently which will make the length of one period of morphology alternation become longer. This is indeed observed in our experiment as we have mentioned before.

VIII. CONCLUSION

In crystallization of NH_4Cl on agar plates, the agar medium plays an important role in impeding the solute transport and promoting the tip splitting. With the mass proportion of agar to NH_4Cl increasing, the aggregate appears as DBM, fractal, and cluster in sequence. On the other hand, with the decrease of growth humidity, supersaturation increases. When the supersaturation exceeds a critical value for kinetic roughening transition, the aggregate transforms from the smooth surface growth type (zigzag pattern, fractal I, cluster I) to the rough one (fractal II, cluster II).

The alternating dense-sparse transitions and the alternating dense-zigzag transitions are determined by the interplay between macroscopic solute transport dynamics and microscopic interfacial growth kinetics. Macroscopically, both of them are transitions between DBM and fractal morphology, and they result from the oscillation of solute concentration in front of the growing interface at a moderate mass proportion. Microscopically, the alternating dense-sparse transitions belong to the rough surface growth and the alternating dense-zigzag transitions are transitions between rough surface growth and smooth surface growth. Which one of them occurs depends on the relative humidity, which controls the supersaturation.

ACKNOWLEDGMENTS

This work was supported by FANEDD of China (Contract No. 200525) and Natural Science Foundation of Hubei Province (Contract No. 5005ABA027). The AFM was performed in Center of Nanoscience and Nanotechnology Research, Wuhan University.

[1] E. Ben-Jacob, R. Godbey, N. D. Goldenfeld, J. Koplik, H. Levine, T. Mueller, and L. M. Sander, Phys. Rev. Lett. **55**, 1315 (1985).
[2] L. Ristroph, M. Thrasher, M. B. Mineev-Weinstein, and H. L. Swinney, Phys. Rev. E **74**, 015201(R) (2006).
[3] L. Niemeyer, L. Pietronero, and H. J. Wiesmann, Phys. Rev. Lett. **52**, 1033 (1984).
[4] M. P. Zorzano, D. Hochberg, M. T. Cuevas, and J.-M. Gómez-Gómez, Phys. Rev. E **71**, 031908 (2005).
[5] J. I. Wakita, H. Shimada, H. Itoh, T. Matsuyama, and M. Matsushita, J. Phys. Soc. Jpn. **70**, 911 (2001).
[6] H. Honjo and S. Ohta, Phys. Rev. A **45**, R8332 (1992).
[7] F. J. Lamelas, S. Seader, M. Zunic, C. V. Sloane, and M. Xiong, Phys. Rev. B **67**, 045414 (2003).
[8] D. Grier, E. Ben-Jacob, R. Clarke, and L. M. Sander, Phys. Rev. Lett. **56**, 1264 (1986).
[9] V. Fleury, W. A. Watters, L. Allam, and T. Devers, Nature (London) **416**, 716 (2002).
[10] M. Wang, X. Y. Liu, C. S. Strom, P. Bennema, W. van Enckevort, and N. B. Ming, Phys. Rev. Lett. **80**, 3089 (1998).
[11] D. W. Li, M. Wang, P. Liu, R. W. Peng, and N. B. Ming, J. Phys. Chem. B **107**, 96 (2003).
[12] E. J. Suárez-Domínguez and J. A. Betancourt-Mar, J. Phys.: Conf. Ser. **23**, 78 (2005).
[13] J. A. Betancourt-Mar and E. J. Suárez-Domínguez, in *Thinking in Patterns: Fractals and Related Phenomena in Nature*, edited by M. M. Novak (World Scientific, Singapore, 2004), p. 311.
[14] M. Yasui and M. Matsushita, J. Phys. Soc. Jpn. **61**, 2327 (1992).
[15] N. Hecker, D. G. Grier, and L. M. Sander, in *Fractal Aspects of Materials*, edited by R. B. Laibowitz, B. B. Mandelbrot, and D. E. Passoja (Materials Research Society, University Park, PA, 1985).
[16] V. Fleury, M. Rosso, and J. N. Chazalviel, Phys. Rev. A **43**, 6908 (1991).
[17] A. Kuhn and F. Argoul, Phys. Rev. E **49**, 4298 (1994).
[18] M.-Q. Lòpez-Salvans, F. Sagués, J. Claret, and J. Bassas, Phys. Rev. E **56**, 6869 (1997).
[19] K. Q. Zhang, M. Wang, S. Zhong, G. X. Chen, and N. B. Ming, Phys. Rev. E **61**, 5512 (2000).
[20] G. Gonzalez, G. Marshall, F. V. Molina, S. Dengra, and M. Rosso, J. Electrochem. Soc. **148**, C479 (2001).
[21] H. Eba and K. Sakurai, J. Electroanal. Chem. **571**, 149 (2004).
[22] M. Wang and N. B. Ming, Phys. Rev. Lett. **71**, 113 (1993).
[23] B. Ratajska-Gadomska and W. Gadomski, J. Chem. Phys. **121**, 12583 (2004).
[24] M. Matsushita, M. Sano, Y. Hayakawa, H. Honjo, and Y. Sawada, Phys. Rev. Lett. **53**, 286 (1984).
[25] T. A. Witten and L. M. Sander, Phys. Rev. Lett. **47**, 1400 (1981).
[26] T. Vicsek, *Fractal Growth Phenomena* (World Scientific, Singapore, 1989).
[27] E. Ben-Jacob and P. Garik, Nature (London) **343**, 523 (1990).
[28] H. K. Henisch, *Crystals in Gels and Liesegang Rings* (Cambridge University Press, Cambridge, 1988).
[29] A. L. Slade, A. E. Cremers, and H. C. Thomas, J. Phys. Chem. **70**, 2840 (1966).
[30] H. Roder, K. Bromann, H. Brune, and K. Kern, Phys. Rev. Lett. **74**, 3217 (1995).
[31] J. Wu, B. G. Liu, Z. Y. Zhang, and E. G. Wang, Phys. Rev. B **61**, 13212 (2000).
[32] T. Michely, M. Hohage, M. Bott, and G. Comsa, Phys. Rev. Lett. **70**, 3943 (1993).
[33] C. H. Claassens, M. J. H. Hoffman, J. J. Terblans, and H. C. Swart, J. Phys.: Conf. Ser. **29**, 185 (2006).
[34] S. Ogura, K. Fukutani, M. Matsumoto, T. Okano, M. Okada, and T. Kawamura, Phys. Rev. B **73**, 125442 (2006).
[35] I. Sunagawa, Forma **14**, 147 (1999).
[36] P. Bennema, J. Phys. D **26**, B1 (1993).
[37] X. Y. Liu, P. van Hoof, and P. Bennema, Phys. Rev. Lett. **71**, 109 (1993).
[38] R. F. Xiao, J. I. D. Alexander, and F. Rosenberger, Phys. Rev. A **43**, 2977 (1991).
[39] S. Gorti, E. L. Forsythe, and M. L. Pusey, Cryst. Growth Des. **5**, 473 (2005).
[40] L. A. Smith, A. Duncan, G. B. Thomson, K. J. Roberts, D. Machin, and G. McLeod, J. Cryst. Growth **263**, 480 (2004).
[41] M. Wang, X. Y. Liu, C. Sun, N. B. Ming, P. Bennema, and W. J. P. van Enckevort, Europhys. Lett. **41**, 61 (1998).
[42] M. Wang and N. B. Ming, Phys. Rev. A **44**, R7898 (1991).
[43] M. Wang and N. B. Ming, Phys. Rev. A **45**, 2493 (1992).